# Radiation hardness characterization of low gain avalanche detector prototypes for the high granularity timing detector
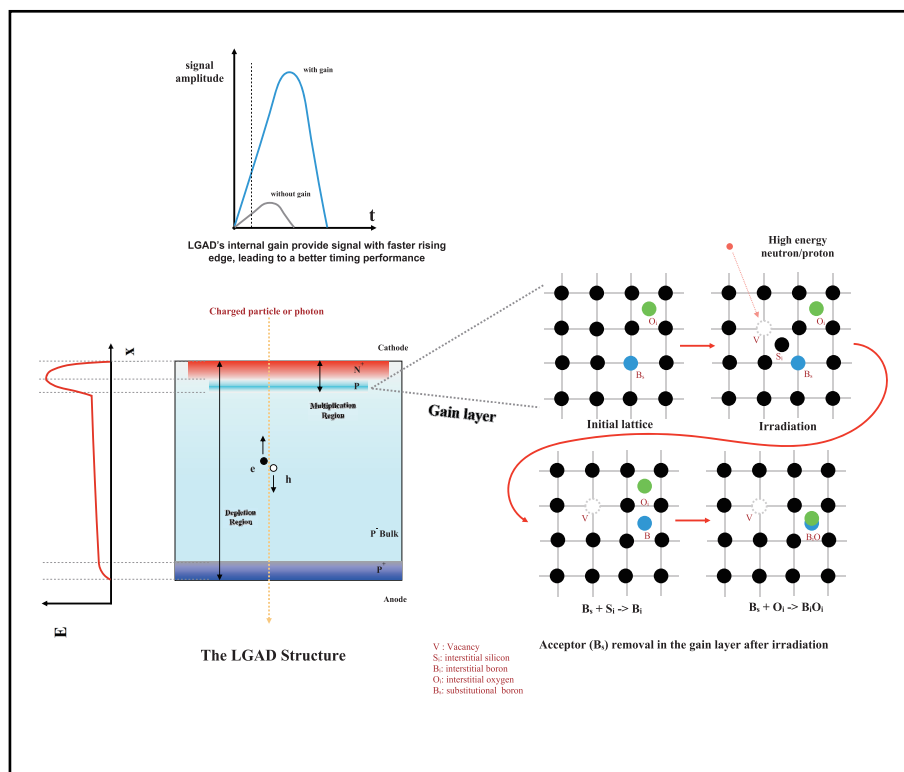
Xiao Yang[1,2], Kuo Ma[1,2], Xiangxuan Zheng[1,2], and Yanwen Liu[1,2] ✉

[1]*Department of Modern Physics, University of Science and Technology of China, Hefei 230026, China;*
[2]*State Key Laboratory of Particle Detection and Electronics, University of Science and Technology of China, Hefei 230026, China*

✉Correspondence: Yanwen Liu, E-mail: yanwen@ustc.edu.cn

## Graphical abstract



*The basic principle and structure of the LGAD technology (left) and the acceptor removal effect (right) for the boron-doped gain layer. The $B_iO_i$ complexes are generated after neutron/proton irradiation, leading to the reduction of the effective doping concentration and detector's gain.*

## Public summary

■ The irradiation effects on both the gain layer and the bulk for prototype LGADs are characterized by *I-V* and *C-V* measurements at room temperature (20 ℃) or −30 ℃.

■ The HPK-1.2 prototype are prove to have the smallest *c*-factor $3.06 \times 10^{-16}$ cm$^{-2}$ and HPK-3.2, USTC-1.1-W8 have larger *c*-factor $3.89 \times 10^{-16}$ cm$^{-2}$, $4.12 \times 10^{-16}$ cm$^{-2}$.

■ A novel analysis method is proposed to further exploit the data to get the relation between the *c*-factor and initial doping density.

# Radiation hardness characterization of low gain avalanche detector prototypes for the high granularity timing detector

Xiao Yang[1,2], Kuo Ma[1,2], Xiangxuan Zheng[1,2], and Yanwen Liu[1,2] ✉

[1]*Department of Modern Physics, University of Science and Technology of China, Hefei 230026, China;*
[2]*State Key Laboratory of Particle Detection and Electronics, University of Science and Technology of China, Hefei 230026, China*

✉Correspondence: Yanwen Liu, E-mail: yanwen@ustc.edu.cn

**Abstract:** The high granularity timing detector (HGTD) is a crucial component of the ATLAS phase II upgrade to cope with the extremely high pile-up (the average number of interactions per bunch crossing can be as high as 200). With the precise timing information ($\sigma_t \sim 30$ ps) of the tracks, the track-to-vertex association can be performed in the "4-D" space. The Low Gain Avalanche Detector (LGAD) technology is chosen for the sensors, which can provide the required timing resolution and good signal-to-noise ratio. Hamamatsu Photonics K.K. (HPK) has produced the LGAD with thicknesses of 35 μm and 50 μm. The University of Science and Technology of China(USTC) has also developed and produced 50 μm LGADs prototypes with the Institute of Microelectronics (IME) of Chinese Academy of Sciences. To evaluate the irradiation hardness, the sensors are irradiated with the neutron at the JSI reactor facility and tested at USTC. The irradiation effects on both the gain layer and the bulk are characterized by *I-V* and *C-V* measurements at room temperature (20 ℃) or −30 ℃. The breakdown voltages and depletion voltages are extracted and presented as a function of the fluences. The final fitting of the acceptor removal model yielded the *c*-factor of $3.06\times10^{-16}$ cm$^{-2}$, $3.89\times10^{-16}$ cm$^{-2}$ and $4.12\times10^{-16}$ cm$^{-2}$ for the HPK-1.2, HPK-3.2 and USTC-1.1-W8, respectively, showing that the HPK-1.2 sensors have the most irradiation resistant gain layer. A novel analysis method is used to further exploit the data to get the relationship between the *c*-factor and initial doping density.

**Keywords:** LGAD; HGTD; timing detector; silicon detectors

**CLC number:** TL814        **Document code:** A

## 1　Introduction

The low gain avalanche detector (LGAD) is a novel detector technology to achieve a timing resolution at the level of 30 ps by adding a gain layer beneath the cathode of the traditional PIN detector[1,2]. This is proposed by the RD50 collaboration[3] inspired by the observed avalanche phenomenon in the heavily hadron irradiated (order of $10^{16}$ cm$^{-2}$ 1 MeV neutron equivalent) silicon detectors. The detector with controlled gain can suppress the jitter noise in timing applications and tolerate extremely high hadron irradiation environment. The successful production of the detector with very thin active detection volume further improves the timing resolution of the LGAD by suppressing the Landau noise. Based on the irradiation hardness and timing resolution, the LGAD technology is chosen by the ATLAS HGTD upgrade project in 2020[4]. Several RD50 member institutes, including CNM, FBK and USTC, have been involved in the optimization of the LGAD design to meet the requirement of the HGTD. The irradiation hardness is studied by the *I-V*/*C-V* measurements of the irradiated sensors at room temperature (20 ℃) and −30 ℃.

The degradation of the performances of silicon detectors is mainly caused by the displacement of the silicon atoms from the lattice sites and the generation of impurities. The defects show up as vacancies, interstitials, or the complex clusters of them. These damages create new energy levels in the band gap. The impact on the characteristics of the sensor can be described by the Shockley-Read-Hall mechanism. The most common macroscopic effects include[5]:

① Increase of the leakage current from the levels close to the mid-gap;

② Increase of the depletion voltage from the levels close to the conduction band;

③ Decrease of the charge collection efficiency by the carrier traps from the deep levels.

For the LGAD detectors the most harmful effect is called the acceptor removal, resulting from the formation of a complex called "B$_i$O$_i$" which have been studied actively by the RD50 collaboration by the deep level transient spectroscopy (DLTS) and thermally stimulated current (TSC) techniques[6]. The appearance of such complex can move the energy level of the original boron acceptors to the donor side and flip the sign of their space charge contribution. As a result, the effective concentration of the boron is reduced, which will decrease the gain of the detector and deteriorate the performance of the sensor[7].

## 2　LGAD samples

The HPK has produced several batches of LGAD prototypes since the very beginning of the HGTD project. Different designs have been studied including different options of the inter-pad gap distance, slim edge technology on the geometry to achieve high fill-factor with good isolation and robustness. Pre-irradiation performances of the first batch HPK LGADs have been reported in Ref.[8]. The radiation campaign has

been described in Ref.[9]. In this work, the irradiation hardness is studied by the *I-V* and *C-V* measurements to extract the information of the gain layer and bulk. Three types of sensors are measured and compared. Two types are from the HPK: Type 1.2 and Type 3.2. They are referred to as HPK-1.2 and HPK-3.2 hereafter. The USTC group has started designing LGAD detector in 2019. The first version (referred to as USTC-1.1 hereafter) has been produced by the IME (Institute of Microelectronics, CAS) in 2020. Samples from the wafer 8 in this production (USTC-1.1-W8) are studied and compared with the HPK sensors in this work. Some design parameters of the sensors are presented in Table 1 and microscope pictures of two sensors are shown in Fig. 1. The pre-irradiation breakdown voltage (VBD) is determined by the voltage when the leakage current of the central pad reach 1 μA during the room temperature *I-V* measurement. The area of the active region is measured with a microscope.

## 3  Methodology

The *I-V* and *C-V* measurements are commonly used to characterize semiconductor detectors. Detector characteristics such as leakage current, break-down voltage, depletion voltages, capacitance at full depletion are important for the operation of the detector and can be determined by the *I-V* and *C-V* curves. The leakage current increases proportionally with the fluences.

$$\Delta I/V = \alpha \Phi_{eq} \qquad (1)$$

where $V$ is the depleted volume, $\Phi_{eq}$ is the fluence, and the $\alpha$-factor is called the current-related damage rate. The $\alpha$-factor decreases with the annealing time. With the standard annealing procedure of a duration of 80 min at 60 ℃, the measured value of $\alpha$ is around $4 \times 10^{-17}$ A·cm$^{-1}$. For the leakage current at different temperatures, the relation with band-gap energy and temperature is followed, leading to

**Table 1.** The main design parameters of the LGAD sensors studied in this work.

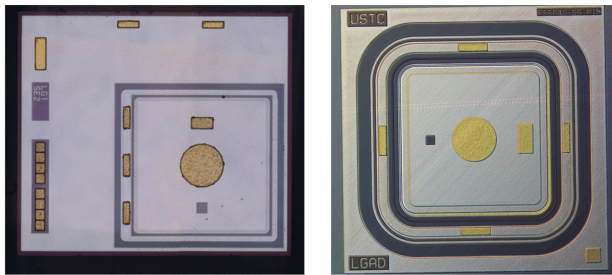| Prototype | Gain layer depth (μm) | Active region | | Pre-irradiation $V_{BD}$ (V) |
| --- | --- | --- | --- | --- |
| | | Area (mm²) | Thickness (μm) | |
| HPK-1.2 | 1 | 1.402 | 35 | 270 |
| HPK-3.2 | 2 | 1.402 | 50 | 130 |
| USTC-1.1-W8 | 1 | 1.000 | 50 | 295 |



**Fig. 1.** Photos of the HPK-1.2 (a) and USTC-1.1-W8 (b) single pad LGAD prototypes tested at USTC.

$$I_{leakage} \propto T_{silicon}^2 \cdot \exp(-E_{eff}/2k_B T_{silicon}).$$

Here, $E_{eff}$ is the band-gap energy, which is 1.21 eV for silicon. For the *C-V* measurement, the following formulae to extract the doping density are reportedly used for p-n junction structures. From electrostatics, the effective doping density can be calculated from the *C-V* curve using

$$N_{eff} = \frac{2}{e\epsilon A^2}\left[\frac{d(C^{-2})}{dV}\right]^{-1}$$

and the depletion depth can be approximated with the planar capacitor formula $w = A\epsilon\frac{1}{C}$ when the concentration of the n side is much higher than the p side. On the curves of $1/C^2$ vs. $V$, as the voltage increases, the slope of the curve will increase drastically when the gain layer is fully depleted, since the doping concentration in the bulk is lower by a few orders of magnitudes than the gain layer. This turning point can be used to measure the gain layer depletion voltage ($V_{GL}$). The $1/C^2$ of the sensor increases with the bias voltage and reaches a constant after the bulk is fully depleted. The voltage required to deplete the bulk ($V_{BK}$) can be approximated by the difference between full depletion voltage ($V_{FD}$) and $V_{GL}$. After irradiation, the defects introduce changes in the space charge region (SCR). The produced energy levels close to the conduction or valence bands create acceptor-like or donor-like effective doping. The effective doping density $N_{eff}$ is related to the fluence $\Phi_{eq}$, as well as the anneal temperature $T$ and time $t$. These changes can be described by the "Hamburg model"[10],

$$\Delta N_{eff}(\Phi_{eq}, t, T) =$$
$$N_C(\Phi_{eq}) + N_A(\Phi_{eq}, t, T) + N_Y(\Phi_{eq}, t, T) \qquad (2)$$

which contains a stable term $N_C(\Phi_{eq})$ representing the modification to the effective doping density by the radiation damage, short term anneal $N_A(\Phi_{eq}, t, T)$ and long term anneal $N_Y(\Phi_{eq}, t, T)$. The stable damage term contains dopant removal and creation terms,

$$N_C(\Phi_{eq}) = N_{C,0}(1 - e^{-c\Phi_{eq}}) + g_c \Phi_{eq} \qquad (3)$$

where $c$ is the initial dopant removal constant, and $g_c$ is the linear induction rate dominating at fluence larger than $1 \times 10^{16} n_{eq}$ cm$^{-2}$[2].

For the characterization of the acceptor removal effect for the p-type gain layer, the contributions from donor term and acceptor generation can be neglected. Eq. (3) can be further simplified into $N_{A,eff} = N_{A,0}e^{-c\Phi_{eq}}$. As the acceptor concentration of the gain layer is proportional to the $V_{GL}$, the $c$-factor can be measured by fitting the curves of $V_{GL}$ vs. $\Phi_{eq}$.

In the following section, the *I-V* and *C-V* measurements are performed with the HPK and USTC sensors. The $\alpha$- and $c$-factors are extracted to evaluate their radiation hardness.

## 4  Results

The HPK-1.2, HPK-3.2 and USTC-1.1-W8 sensors are irradiated to the fluences of $8 \times 10^{14}$, $1.5 \times 10^{15}$, $2.5 \times 10^{15}$, $3 \times 10^{15}$, $6 \times 10^{15}$ cm$^{-2}$ 1 MeV neutron equivalent at JSI neutron reactor[11]. Some fluence points are missing for a few samples due to the availability of fluences in each campaign. All irradiated samples are annealed with the RD50 standard procedure of 60 ℃ for 80 min[12].

The measured *I-V* curves are shown in Fig. 2. For HPK-1.2 and HPK-3.2 samples, the *I-V*s are measured at room temper-

(a) HPK-1.2(room temperature)



(b) HPK-3.2(room temperature)



(c) USTC-1.1-W8(room temperature)



(d) USTC-1.1-W8(T=−30 ℃)

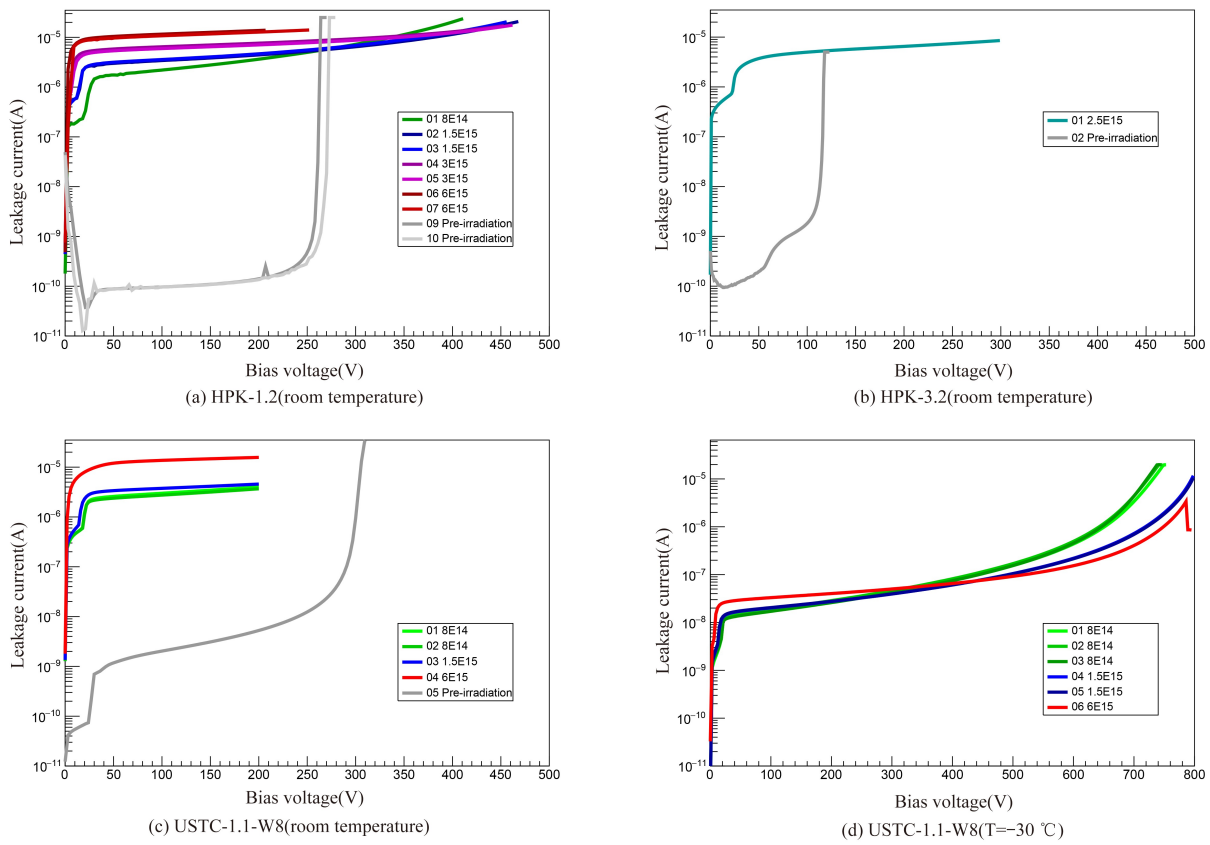**Fig. 2.** *I-V* results of the HPK-1.2, HPK-3.2 and USTC-1.1-W8 LGADs at difference fluences. The measurements are preformed at $T$ = 20 ℃ (room temperature) for all samples and $T$ = −30 ℃ for USTC sensors with guard rings grounded.

ature to obtain the $\alpha$-factor to study bulk damage. The USTC-1.1-W8 samples are measured at −30 ℃ to find the operation voltages for HGTD upgrade. As we can see from the curves of the HPK-1.2 and HPK-3.2, the leakage current after gain layer depletion increases as the fluences increase. To guarantee the gain layer depletion and reduce the effect of the gain, the leakage current at 68 V is used to calculate the $\alpha$ with Eq. (1). The $\Delta I/V$ is plotted as a function of fluences (Fig. 3) and the $\alpha$ is obtained by the linear fit of the curve. As shown in the figure, the linear function fits well the data and the $\alpha$-factor is $3.64 \times 10^{-17}$ A·cm$^{-1}$ for HPK-1.2, $3.89 \times 10^{-17}$ A·cm$^{-1}$
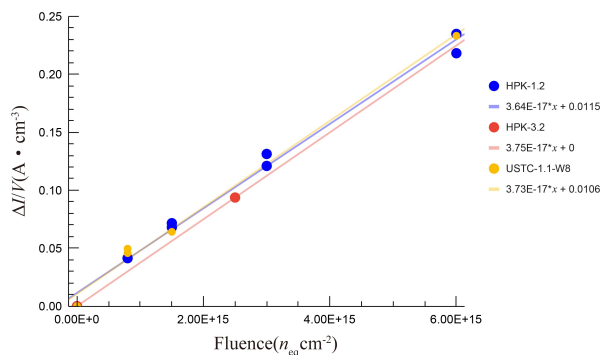


**Fig. 3.** The $\Delta I/V$ at different fluences calculated from Room T. *I-V* for HPK-1.2, HPK-3.2 and USTC-1.1-W8 sensors used to estimate the $\alpha$-factor representing the damages generated in the bulk region.

for HPK-3.2 and $3.73 \times 10^{-17}$ A·cm$^{-1}$ for USTC-1.1-W8, respectively. The results agree with the result from DESY's previous study: $4 \times 10^{-17}$ A·cm$^{-1}$[13, 14].

The measured *C-V* curves are shown in Fig. 4. The effective doping densities for the USTC-1.1-W8 sensors are derived using the formulae explained above and are presented in Fig. 5. The acceptor removal effect can be clearly seen. The $V_{GL}$ is obtained from the $1/C^2$-$V$ curves for each type of the sensors at different fluences by extrapolating the line fitted from the rising region on $1/C^2$-$V$ and finding its intersection with the x-axis. The obtained value are summarized in Table 2. The prototypes which have more than one samples available for a same fluence are measured separately on $V_{GL}$ and the averaged values are shown. The measured $V_{GL}$ as a function of fluences are shown in Fig. 6. The exponential fit are performed for each prototype and the results are shown in the plot according to the acceptor removal model. The fraction of the active acceptor remained estimated from $V_{GL}$ changes are shown in Fig. 7, from which we can see the significant degradation of active acceptors after $1 \times 10^{15} n_{eq}$ cm$^{-2}$ fluence. At the end, the derived $c$-factor is $3.06 \times 10^{-16}$ cm$^2$ for HPK-1.2, $3.89 \times 10^{-16}$ cm$^2$ for HPK-3.2 and $4.12 \times 10^{-16}$ cm$^2$ for USTC-1.1-W8. The acceptor removal $c$-factors and $\alpha$-factors are shown compared in Table 3. The results indicated that the HPK-1.2 have better gain layer radiation hardness compared to the HPK-3.2, and the HPK-3.2 is a slightly better than USTC-1.1-W8.
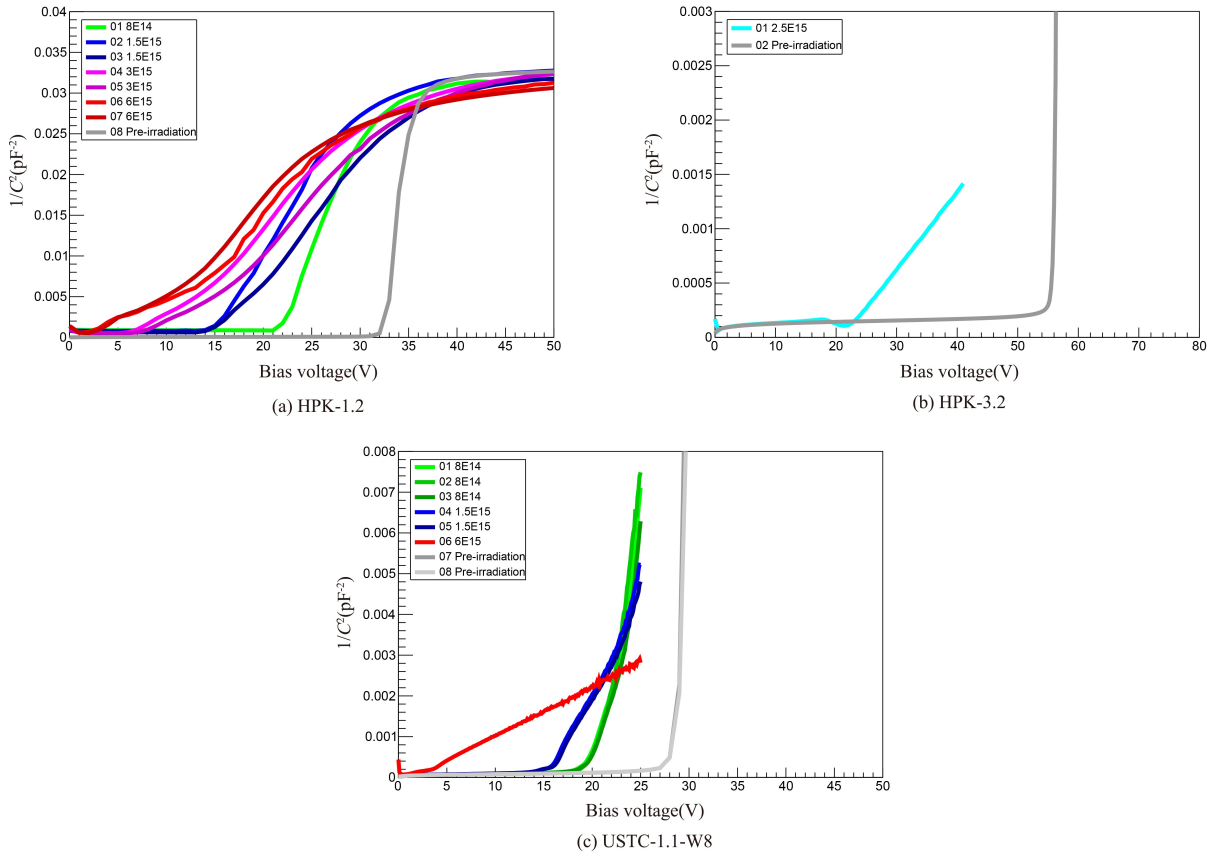
(a) HPK-1.2



(b) HPK-3.2



(c) USTC-1.1-W8

**Fig. 4.** $1/C^2$ -$V$ of the HPK-1.2, HPK-3.2 and USTC-1.1-W8 LGADs at difference fluences. The measurements are preformed at $T = 20$ ℃, with guard rings grounded.
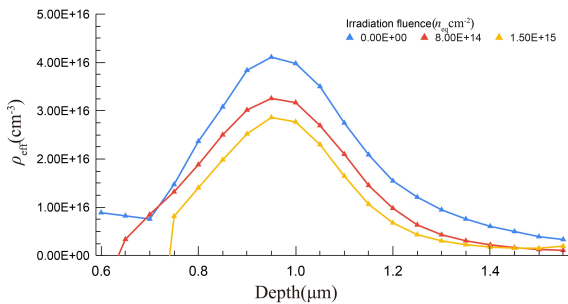


**Fig. 5.** The doping profile before and after 8E+14, 1.5E+15 irradiation fluences of USTC-1.1-W8 LGAD samples. The doping density of each point is calculated by the average of the doping densities from the samples with the same fluence and average the results in each interval to suppress the fluctuation.
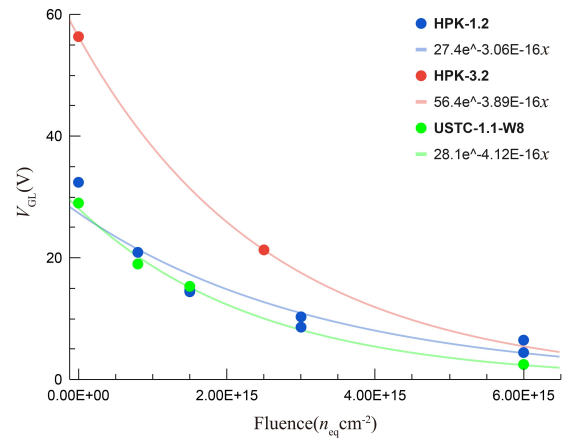
**Table 2.** $V_{GL}$ of the sensor prototypes at different fluences measured at room temperature used to determine the $c$-factor. The '-' signs correspond to the missing fluence points.

| Fluences ($10^{15}$ 1 MeV $n_{eq}$ cm$^{-2}$) | $V_{GL}$ at different fluences (V) | | | | | |
|---|---|---|---|---|---|---|
| | 0 | 0.8 | 1.5 | 2.5 | 3.5 | 6 |
| HPK-1.2 | 32.41 | 20.90 | 14.56 | — | 9.45 | 5.45 |
| HPK-3.2 | 56.35 | — | — | 21.30 | — | — |
| USTC-1.1-W8 | 29.00 | 18.98 | 15.31 | — | — | 2.48 |



**Fig. 6.** $V_{GL}$ as a function of fluences of all prototypes tested.

With the formulas introduced in Section 3, we reconstructed the effected doping profile of the gain layer with the measured $C$-$V$ data from USTC-1.1-W8 at the fluences of 0, $8 \times 10^{14} n_{eq}$ cm$^{-2}$ and $1.5 \times 10^{15} n_{eq}$ cm$^{-2}$ shown in Fig. 5. The doping density of each point is calculated by the average of the doping densities from the samples with the same fluence and average the results in each interval to suppress the fluctuations. Comparing the curves at different fluences we can clearly see the degradation of the active acceptor density in the gain layer due to the acceptor removal effect.

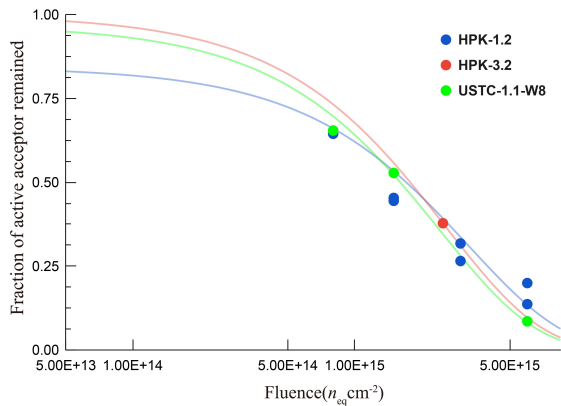Since the acceptor removal $c$-factor have the dependency

**Fig. 7.** Fraction of active acceptor dose changes with fluences measured from the room-temperature *C-V.* is shown as a function of fluences. The active acceptor density degrades significantly after 1E + 15.

**Table 3.** Summary of the $\alpha$-factors and $c$-factors of different sensors.

| Prototype | $c$ ($10^{-16}$ cm$^2$) | $\alpha$ ($10^{-17}$ A·cm$^{-1}$) |
|-----------|------------|------------|
| HPK-1.2 | 3.06 | 3.64 |
| HPK-3.2 | 3.89 | 3.75 |
| USTC-1.1-W8 | 4.12 | 3.73 |

on the initial acceptor density. We computed the local $c$-factor based on the doping profile curves in Fig. 5 by performing the exponential fitting on the data at each given depth on the three curves. To eliminate the edge effects during the $N_{eff}$ calculation, only the data in the range from 0.85 to 1.5 μm are considered in further analysis. The obtained $c$-factors are plotted as a function of the initial acceptor density for each depth the curves are shown in Fig. 8. The results show that the $c$-factor gets smaller with higher acceptor density, which agrees with the conclusion from previous study that higher initial acceptor density will improve the irradiation hardness[15]. To make the result more quantitative, a logarithm fit is performed on the result and $c(10^{-16}\cdot\text{cm}^2) = -2.98\cdot\ln(\rho_0(\text{cm}^{-3})) + 117$. The fitted function follows fairly well the data points. A function like this can be used to predict the evolution of the doping profile as the LGAD accumulates fluences, which can be
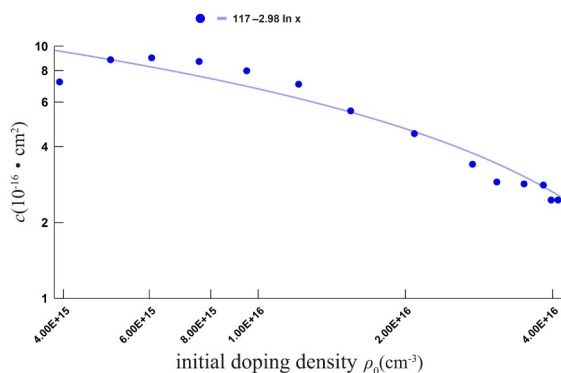
an important tool for the sensor design. The modelling of the dependence is still primitive and should be improved with more measurements and analyses.

# 5   Conclusions

The LGAD detector technology features a controlled internal gain realized by a high doping concentration of Boron beneath the p-n junction. The *I-V* and *C-V* measurements can be used to characterize the sensors. The *V* are measured by USTC for the HGTD prototype sensors irradiated to different fluences. The radiation hardness is assessed by the $\alpha$-factors for bulk, and $c$-factors for gain layer. The results shows the HPK-1.2 have the smallest $c$-factor $3.06 \times 10^{-16}$ cm$^{-2}$, and HPK-3.2, USTC-1.1-W8 have larger $c$-factor $3.89\times10^{-16}$ cm$^{-2}$, $4.12 \times 10^{-16}$ cm$^{-2}$. A novel analysis method is designed to study the dependence of the $c$-factor on the initial doping density, and an expected trend is observed. The result can help the optimization of the gain layer design and the method will be applied and will be further developed with more measurements and analyses in the future.

# Acknowledgments

# Conflict of interest

The authors declare that they have no conflict of interest.

# Biographies

**Xiao Yang** received the BE degree in the physics from the University of Science and Technology of China (USTC) in 2018, and currently working toward the PhD degree in experimental particle physics in the USTC. His research interests include development and characterization of radiation hard silicon sensors used for the high energy particle detection in physics experiment in LHC including TCAD simulation and fabrication process and the standard model Higgs properties study in the ATLAS experiment including Higgs associated production with a vector boson and decay into a pair of W bosons.

**Yanwen Liu** is currently a Full Professor at the University of Science and Technology of China (USTC). He received the PhD from the University of Geneva in 2004 (with the CDF experiment), and worked at Universite Catholique de Louvain in Belgium in 2005 as a postdoc (with the CMS experiment) before he joined the USTC. Since then, he worked on physics analyses at Dzero and ATLAS experiments (H->gamma gamma, bb, electroweak measurements, and search for new physics beyond the SM). His current research activities include development of Low Gain Avalanche Detector for High Granularity Timing Detector, a phase-II upgrade project for ATLAS as well as physics studies with the ATLAS data.



**Fig. 8.** The $c$-factor as a function of initial doping density ($\rho_0$) measured from USTC-1.1-W8 irradiated samples.

# References

[1] Pellegrini G, Fernández-Martínez P, Baselga M, et al. Technology developments and first measurements of Low Gain Avalanche Detectors (LGAD) for high energy physics applications. *Nuclear Instruments and Methods in Physics Research A,* **2014**, *765*: 12–16.

[2] Hartmann F. Evolution of Silicon Sensor Technology in Particle Physics. Berlin: Springer, 2017. https://linkspringer.53yu.com/book/10.1007%2F978-3-319-64436-3.

[3] Rd50 collaboration. RD50 - Radiation hard semiconductor devices for very high luminosity colliders. http://rd50.web.cern.ch/rd50.

[4] Lanni F, Pontecorvo L. Technical design report: A high-granularity timing detector for the ATLAS Phase-Ⅱ Upgrade, Geneva, Switzerland: CERN, 2020.

[5] Rossi L, Fischer P, Rohe T, et al. Pixel Detectors: From Fundamentals to Applications. Berlin: Springer, 2006. https://xs.dailyheadlines.cc/books?hl=zh-CN&lr&idJbp73yTz-LYC&oifnd&pgPA1&dqRossi+L,+Fischer+P,+Rohe+T,+et+al.+Pixel+Detectors:+From+Fundamentals+to+Applications.+Berlin:+Springer,+2006.&otsYHP700x7Gt&sigOxQfRU9rZumpdGwcgDKyBxDQHYc.

[6] Gurimskaya Y, de Almeida P D, Garcia M F, et al. Radiation damage in p-type EPI silicon pad diodes irradiated with protons and neutrons. *Nuclear Instruments and Methods in Physics Research A,* **2020**, *958*: 162221.

[7] Jin Y, Ren H, Christie S, et al. Experimental study of acceptor removal in UFSD. *Nuclear Instruments and Methods in Physics Research A,* **2020**, *983*: 164611.

[8] Yang X, Alderweireldt S, Atanov N, et al. Layout and performance of HPK prototype LGAD sensors for the High-Granularity Timing Detector. *Nuclear Instruments and Methods in Physics Research A,* **2020**, *980*: 164379.

[9] Shi X, Ayoub M K, Cui H, et al. Radiation campaign of HPK prototype LGAD sensors for the High-Granularity Timing Detector (HGTD). *Nuclear Instruments and Methods in Physics Research A,* **2020**, *979*: 164382.

[10] Moll M. Radiation damage in silicon particle detectors. Hamburg, Germany: Hamburg University, 1999: DESY Thesis-1999-040. https://www.osti.gov/etdeweb/biblio/20033260.

[11] Snoj L, Ambrožič K, Čufar A, et al. Radiation hardness studies and detector characterisation at the JSI TRIGA reactor. *EPJ Web of Conferences,* **2020**, *225*: 04031.

[12] Moll M. Radiation damage and annealing in view of QA aspects. In: 1st Workshop on Quality Assurance Issues in Silicon Detectors. Geneva, Switzerland: CERN, 2001. http://ssd-rd.web.cern.ch/qa/talks/Michael_Moll-QA-2001.pdf.

[13] Wunstorf R. Systematic Studies on the Radiation Resistance of Silicon Detectors for the Application in High-Energy Physics Experiments. Hamburg, Germany: Deutsches Elektronen-Synchrotron (DESY), 1992. https://inis.iaea.org/search/search.aspx?orig_q=RN:24030522.

[14] Moll M, Fretwurst E, Lindström G, et al. Leakage current of hadron irradiated silicon detectors-material dependence. *Nuclear Instruments and Methods in Physics Research A,* **1999**, *426*: 87–93.

[15] Ferrero M, Arcidiacono R, Barozzi M, et al. Radiation resistant LGAD design. *Nuclear Instruments and Methods in Physics Research A,* **2019**, *919*: 16–26.